ARTICLES
https://doi.org/10.1038/s43588-020-00001-y

nature computational science

Stable maintenance of hidden switches as a strategy to increase the gene expression stability

Hiroyuki Kuwahara and Xin Gao ✉

In response to severe genetic and environmental perturbations, wild-type organisms can express hidden alternative phenotypes adaptive to such adverse conditions. While our theoretical understanding of the population-level fitness advantage and evolution of phenotypic switching under variable environments has grown, the mechanism by which these organisms maintain phenotypic switching capabilities under static environments remains to be elucidated. Here, using computational simulations, we analyzed the evolution of gene circuits under natural selection and found that different strategies evolved to increase the gene expression stability near the optimum level. In a population comprising bistable individuals, a strategy of maintaining bistability and raising the potential barrier separating the bistable regimes was consistently taken. Our results serve as evidence that hidden bistable switches can be stably maintained during environmental stasis—an essential property enabling the timely release of adaptive alternatives with small genetic changes in the event of substantial perturbations.

The capacity to buffer genetic variations and express similar phenotypes is thought to be a general property of naturally selected organisms[1–6]. Substantial perturbations in a wild-type organism can, however, disrupt the normal working of its genetic developmental system and express alternative phenotypes that would not otherwise be expressed[7–11]. To release such cryptic phenotypes, wild-type organisms somehow maintain phenotypic switching capabilities and lower the threshold of the switch in response to severe perturbations. The stable maintenance of such 'hidden' threshold traits in naturally selected organisms suggests that loss of these obsolete switching mechanisms somehow incurs fitness costs and is detrimental to the organisms, which could be attributed to, for example, pleiotropic effects on expressed phenotypes[12]. However, gene sets associated with cryptic phenotypes are likely to be unexpressed under normal conditions and do not seem to contribute to an organism's fitness. Thus, although the presence of phenotypic switching capabilities is commonly presumed in wild-type organisms, it remains elusive exactly how disused mechanisms can be beneficial and maintained in a population for extended periods[12,13].

Here, using computational simulations, we report that evolutionary directions towards high gene expression stability can explain the stable maintenance of obsolete switching capabilities under natural selection. We simulated the evolution of a gene circuit model that has the potential to exhibit a bistable switch. During in silico evolution, we placed the population of organisms in a static environment with selection towards an intermediate optimum (that is, stabilizing selection), then in a fluctuating environment and, lastly, back in the static environment. We observed that a bistable trait evolved in the fluctuating environment to exhibit stochastic switching had a high likelihood of being maintained in the population in the subsequent static environment. We found that the bistable trait evolved in the fluctuating environment had contrasting characteristics to the one maintained in the subsequent static environment; whereas the former had a low-threshold switch to ensure that a small fraction of the population could adapt to the adverse environment (that is, could be used for stochastic switching), the latter had a higher-threshold switch to reduce gene expression variability (that is, could be used to increase gene expression stability). Our results provide evidence for the establishment and maintenance of such hidden switching capabilities in a static environment. Interestingly, this is not because bistable switching has selective advantages under stabilizing selection, but because increasing the barrier between the stable states is an easier solution to incrementally increase the stability of gene expression with small mutational shifts rather than reverting to a monostable gene expression system.

Results

Gene circuit model and evolutionary simulation. We simulated the evolution of a population of 1,000 asexual microorganisms in varying environmental conditions. We represented each individual organism in the population by a stochastic gene circuit model regulating the expression of master regulatory protein X. The gene circuit model for the expression of protein X comprised four reaction processes: transcription, messenger RNA degradation, translation and protein degradation. This model has four evolvable parameters: a, transcriptional efficiency; b, translational efficiency (or protein burst size); K_d, binding affinity (or the activation threshold); and n, binding cooperativity. In this simulation, the individuals in the founding population were isogenic and had identical, monostable gene circuits based on a constitutive promoter without feedback loop (that is, $n=0$).

We based the selection of individuals in the population on the expression of X and allowed the circuitry to form a positive-feedback loop, which could give rise to a bistable switch with the correct combination of parameters. We had two different environments E_0 and E_1 with different selective pressures. Environment E_0 favored lower expression levels of protein X, whereas environment E_1 favored higher expression levels considering metabolic costs for the protein production (that is, stabilizing selection towards a given optimal expression level).

In the simulation, the population underwent evolution for 90,000 generations under different conditions. During the first 30,000 generations, we placed the population in E_1 and named the evolved

Computational Bioscience Research Center (CBRC), Computer, Electrical and Mathematical Sciences and Engineering (CEMSE) Division, King Abdullah University of Science and Technology (KAUST), Thuwal, Saudi Arabia. ✉e-mail: xin.gao@kaust.edu.sa

population in this first environmental condition as the ancient population. For the next 30,000 generations, we placed the population in a fluctuating environment that switched environments between E_0 and E_1 every 20 generations and named this population as the intermediate population. Finally, during the last 30,000 generations, we placed the population back in E_1 and named the evolved population in this environmental condition as the derived population. We generated 200 sample evolutionary trajectories from this simulation procedure.

Phenotypic characteristics determined by the environment. We analyzed the fitness and phenotypic characteristics of the ancient, intermediate and derived populations. To this end, we measured the mean and standard deviation of the fitness and the protein abundance level from 200 sample trajectories for each population (Supplementary Fig. 1). Because the ancient and derived populations evolved in E_1 over a long period of generations, we expected these populations to be highly adapted to this static environment. In contrast, we expected the intermediate population to experience more difficulties in adapting under fluctuating selection. Unsurprisingly, we observed that the ancient and derived populations had very high average fitness with low variances, while the intermediate population had lower average fitness with higher variances (Supplementary Fig. 1a).

The protein abundance distribution data also showed distinct differences between the populations evolved in the static and fluctuating environments (Supplementary Fig. 1b). Although both ancient and derived populations had similar and consistent protein distributions around the optimum level, the intermediate population had widespread phenotypic patterns with consistently lower protein abundance levels. Many of the samples of the intermediate population had a high variance-mean ratio, indicating that they had high phenotypic variability. This was expected because such a high level of phenotypic variability is advantageous in fluctuating environments and could arise from heterogeneous populations or more homogeneous populations with stochastic switching capability[14–21].

Genotypic differences between ancient and derived populations. There are two possibilities for the derived population to attain phenotypic characteristics resembling those of the ancient population; it could either take the reversion course to attain genotypes similar to those of the ancient population or evolve in a new direction to have novel genotypes optimized for E_1. To distinguish between these possibilities, we compared evolved parameters representing the most common genotype in the derived population with those in the ancient and intermediate populations (Fig. 1). The comparison of evolved parameters between the ancient and derived populations revealed weak correlations, indicating that the evolved genotypes in the derived population were widely different from those in the ancient population (Fig. 1a).

What caused the genotypic differences between the ancient and the derived populations? The only difference between the two populations in our simulation was the initial genotypes; the derived population inherited genotypes from the intermediate population, whereas the ancient population started with a homogeneous genotype exhibiting monostable gene expression. Thus, the genotypes that evolved in the fluctuating environment must have played a crucial role in directing the derived population to follow a different strategy and form novel genotypes optimized for E_1. Indeed, the evolved parameters in the derived population showed far stronger positive correlations with those in the intermediate population (Fig. 1b).

To examine how the genotypes of the intermediate population contributed to the evolution of novel genotypes in the derived population, we analyzed the distribution of each evolvable parameter in the three populations (Fig. 2c). The strongest pattern that emerged from this was that the intermediate and derived populations had high levels of binding cooperativity (that is, high values of n), indicating highly nonlinear transcription processes with strong positive feedback, whereas the ancient population had very low levels of binding cooperativity (that is, low values of n).

Maintenance of bistability under the stabilizing selection. Because nonlinear transcription with strong positive feedback can give rise to bistability and stochastic phenotypic switching[22], we examined the shape of protein abundance level distributions for the evolved individuals and classified their gene regulatory processes as monostable or bistable. To this end, we analyzed the evolved parameter sets for bistability and counted the number of populations with at least one individual with the bistable trait (Fig. 2a). We found that the two populations evolved in the static environment had widely different characteristics of gene expression control ($P < 10^{-21}$ with a two-sided Fisher's exact test). Whereas the bistable trait was rarely observed in the ancient population as expected (3.5%: 7 of 200 samples), the derived population repeatedly expressed the bistable trait (65%: 131 of 200 samples), with bistable individuals often accounting for the majority of the population (77%: 101 of 131 samples) (Supplementary Fig. 2). Because bistability was highly prevalent in the intermediate population (73%: 146 out of 200 samples), we analyzed the extent to which the intermediate population plays a role in the expression of the bistable trait in the derived population (Fig. 2b). In the 131 samples in which the derived population showed bistability, more than 85% were associated with the development of bistability in the intermediate population. To quantify the degree of association between the intermediate and derived population, we constructed a confusion matrix classifying the two populations by the number of monostable and bistable samples (Fig. 2c). We found that the derived population was strongly associated with the intermediate population (odds ratio (OR) = 46.1, 95% confidence interval (CI) = [17.0, 148.6]; $P < 10^{-25}$ with a two-sided Fisher's exact test).

To further test the strong positive association between the intermediate population and bistability in the derived population, we performed additional 200 evolutionary simulations, changing only the epoch of each of the three environmental phases to 10,000 generations (Supplementary Fig. 3). This allowed us to compare the prevalence of bistability in the populations evolved for 30,000 generations with and without the intermediate fluctuating selection phase. First, we analyzed the association between the intermediate and derived populations from these simulation results (Supplementary Fig. 4) and confirmed that the two populations had a strong positive association (OR = 225.1, 95% CI = [65.3, 1024.2]; $P < 10^{-25}$ with a two-sided Fisher's exact test). Next, using the main simulation results of the ancient population, which evolved in E_1 for 30,000 generations, as negative controls, we assessed the degree to which the presence of an intermediate fluctuating selection phase influenced the prevalence of bistability in populations evolved for 30,000 generations (Supplementary Fig. 5). The results showed that the intermediate fluctuating selection phase had a strong positive relation with the prevalence of bistability in the derived population (OR = 24.7, 95% CI = [11.0, 65.5]; $P < 10^{-25}$ with a two-sided Fisher's exact test). These results strongly indicate that bistability that evolved in the intermediate population has a high likelihood of being maintained in the derived population.

To test whether these results depended strongly on our specific choice of simulation settings, we performed additional evolutionary simulations with different settings and analyzed the correlation between the derived and intermediate populations (Supplementary Section 1 and Supplementary Figs. 6–10). These additional experiments confirmed the consistency of our qualitative results under various evolutionary simulation settings.

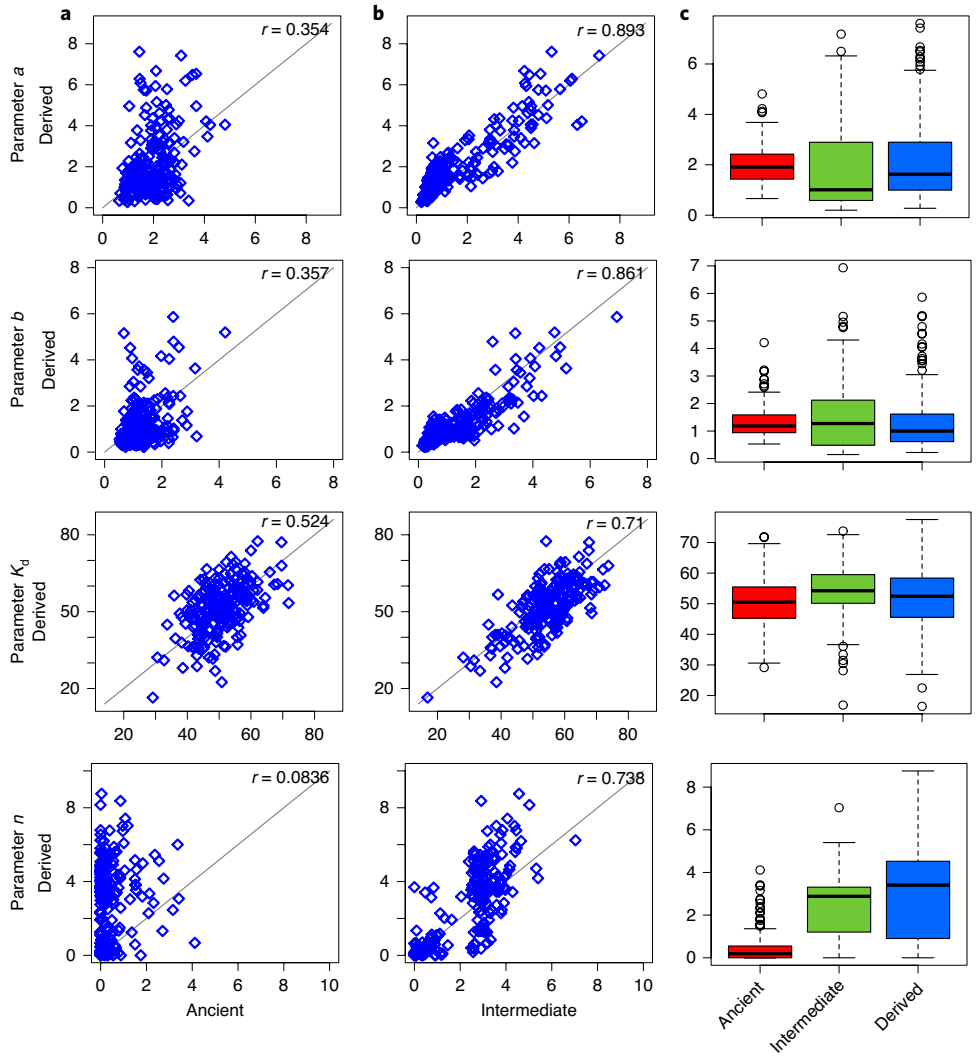

Fig. 1 | Comparison of genotypic characteristics among different phases. a,**b**, Scatter plots showing the four evolved parameters for the most common genotype in the ancient and derived populations (**a**) and the intermediate and derived populations (**b**). **c**, Boxplots showing the statistics of the most common genotype in the three evolved populations (center line, median; box limits, upper and lower quartiles; whiskers, 1.5× interquartile range; points, outliers). The evolved parameters in the ancient, intermediate and derived populations are from the 30,000th, 29,900th and 30,000th generations, respectively.

Increased expression stability under stabilizing selection. How could the bistable trait evolved in the intermediate population be stably maintained in the derived population? Under fluctuating selection, bistability and stochastic phenotypic switching could evolve as a by-product to increase evolvability[21]. Because stochastic switching allows a fraction of individuals to adapt to adverse environments without genetic mutations, the population can increase the overall fitness rapidly[23–26]. Thus, we expected such a strategy, once evolved, to be fixated in the intermediate population. In the static environment, however, random switching between the alternative phenotypes would result in unfit individuals without any obvious advantages. That is, under stabilizing selection, more advantageous characters would be those with high gene expression stability to constantly express optimized phenotypes[27].

Thus, we suspected that the direction of evolution in the static environment was associated with an increase in the stability of gene expression process near the optimal level. One mechanism to lower gene expression noise (that is, increase the gene expression stability) is to increase transcriptional efficiency and to decrease translational efficiency[14,28]. Interestingly, we observed that the ancient population evolved higher transcriptional efficiency (that is, higher levels of a) and lower translational efficiency (that is, lower levels of b) once the gene expression rate approached the optimal level (Supplementary Fig. 11). This showed that individuals with higher gene expression stability were selected for in the ancient population. However, we were not able to detect similar strong patterns for higher gene expression stability in the derived population (Supplementary Fig. 11). This may be due to a more complex relation between the gene regulation parameters and the dynamical behavior given the higher levels of nonlinearity.

To better understand the relation between the gene expression stability and the evolution under stabilizing selection, we quantified the stability level of the gene expression process in the individuals in the ancient and the derived populations. To this end, we defined a stability measure around the higher-expression stable state by assuming that the distribution of the protein abundance around the stable state was well approximated by a Gaussian function. This stability measure is general and can be used to quantify the gene expression stability of different types of regulation. For instance, evolutionary simulation of a negative feedback gene circuit under stabilizing selection showed a gradual increase in the stability level (Supplementary Fig. 12).

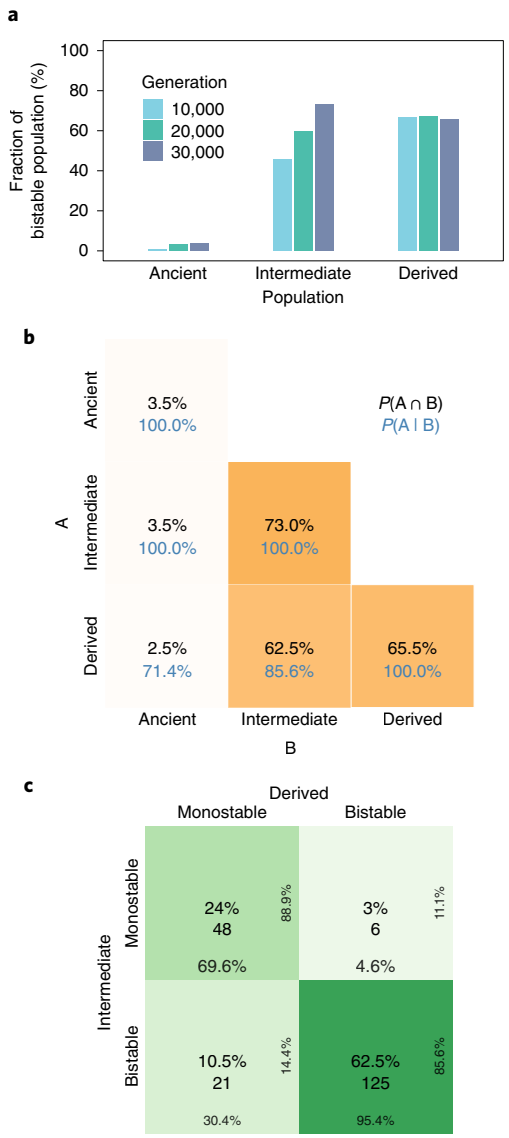

Fig. 2 | Association of bistable populations from different phases. **a**, Fraction of bistable populations at the 10,000th, 20,000th and 30,000th generations in the three different phases. **b**, Joint and conditional probabilities of bistability among the three evolved populations. **c**, A confusion matrix showing the number of monostable and bistable populations in the intermediate and the derived phases. In each cell, the percentage value in the middle shows the normalized count and the whole value underneath shows the absolute count. The row- and column-wise normalized counts are shown in a smaller font size.

Using this stability measure, we computed the time evolution of the mean stability level from the 200 sample trajectories (Fig. 3a). As expected, we found that the ancient and derived populations both increased their stability levels as they evolved. Interestingly, we found that the mean stability level was higher in the derived population, suggesting that nonlinearity and bistability evolved in the derived population had beneficial effects on the stability level. To seek further clarification, we analyzed differences in the increase in the stability level between the monostable and bistable populations. We partitioned 200 samples of the derived population based on the number of stable states and compared their average stability levels to those of the corresponding intermediate population evolved in the E_1 epoch (the intermediate population at 29,900 generations). In an overwhelming majority (196 of 200 samples), the average stability level was higher in the derived population than in the intermediate population (Fig. 3b). Although this was expected as the derived population was evolved in E_1 for a higher number of generations, the increase in the stability level was higher with the bistable trait (Fig. 3b), suggesting that bistability is more advantageous under stabilizing selection.

Next, we examined the mechanism by which gene expression stability evolved in the static environment. We measured the potential landscape of the gene expression process of the fittest individuals. We found that, although a wide variety of monostable and bistable individuals evolved in the derived population, they shared a common phenotypic character that deepened the potential well around the stable state to increase the gene expression stability in the vicinity of the optimal level (Fig. 3c,d).

To further test the beneficial effects of bistability on increasing the stability level, we performed additional simulations by changing the mutation rate and the environmental switching rate settings as the right combinations of these parameters were thought to be crucial for evolutionary strategies to cope with fluctuating environments[21,29,30]. Results from these additional simulations suggest that the maintenance of bistability under stabilizing selection is advantageous for increasing the gene expression stability level (Supplementary Section 2 and Supplementary Figs. 13 and 14).

Maintenance of bistability as a general strategy. To evaluate whether the maintenance of the bistable trait to increase the gene expression stability is a general strategy that is independent of the specific structure of underlying gene circuit models, we used a more general model based on Gaussian distributions. This abstract model represents a monostable gene expression process using a Gaussian distribution and a bistable one using a mixture of two Gaussian distributions. Transitions between the monostable and bistable processes are modeled using the Gaussian width. Using evolutionary simulation, we fixed the stable state of each gene expression model to a level relatively close to the optimal one under stabilizing selection, interpreting changes in the gene expression stability through changes in the value of the Gaussian width. Such a Gaussian distribution-based model—reported to be general and realistic—has been used to analyze the role of gene expression noise in adaptive evolution in yeast[31].

We used these Gaussian-based monostable and bistable expression models to simulate the evolution of clonal monostable and bistable founders under stabilizing selection. We performed simulations with different fitness functions, initial Gaussian widths and optimum expression levels and found that in all simulation settings, the Gaussian width consistently decreased, indicating that the gene expression stability increased as the population evolved (Fig. 4a and Supplementary Figs. 15–17). These results also showed that, when the founding population comprised monostable individuals, the monostable trait was maintained to incrementally increase the gene expression stability. This was expected because increasing the stability of the high-expression stable state would decrease the number of monostable individuals with lower fitness, which in turn would increase the population fitness. When the founding population comprised bistable individuals, we observed the evolution of higher gene expression stability and maintenance of the bistable trait, which is consistent with the results of our positive-feedback gene circuit model.

To examine the selection mechanism for narrower Gaussian widths in both monostable and bistable models, we computed the average fitness for a range of combinations of the high-expression stable state and the Gaussian width (Fig. 4b). We found that the effects of narrower Gaussian widths to increase the average fitness were larger in the bistable model, indicating that higher stability levels are more advantageous in the bistable trait than in the monostable trait. This is consistent with the stability level results (Fig. 3a)

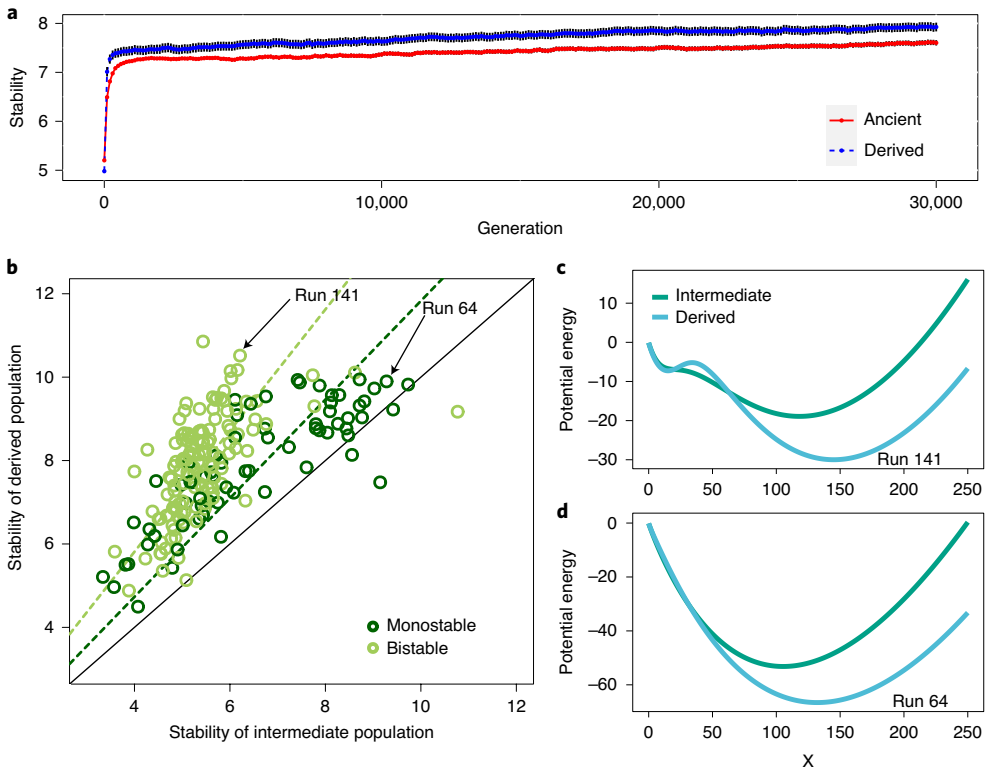

Fig. 3 | Evolution of gene expression stability. a, Mean evolution of the average stability around the higher-expression stable state between the ancient and derived populations over the 200 evolutionary simulation runs. The error bars show the s.e.m. **b**, The average stability around the higher-expression stable state between the evolved individuals in the intermediate and derived populations. Each dashed line represents a regression line with zero intercept for the group with the corresponding color. The slope of the line is 1.453 for bistable populations and 1.183 for the monostable populations. **c**,**d**, A change in the potential function of the fittest individual in the intermediate and derived populations for a sample run producing a bistable derived population (**c**) and a monostable derived population (**d**). The *x* axis shows the abundance level of protein X.

and is justifiable because a wider Gaussian width results in a higher chance of the system moving spontaneously to the lower-expression stable state regime in the bistable model, which in turn lowers the average fitness. These results indicate that while mutational shifts to increase stability levels are advantageous in both monostable and bistable traits under stabilizing selection (Fig. 4c), the benefit is more pronounced in the bistable trait.

Discussion

In this computational study, we first focused on adaptive evolution of positive-feedback gene circuits under stabilizing selection and made several assumptions. For example, we modeled transcription regulation by assuming the interaction between the transcription factor and the operator site to be in equilibrium. Although this thermodynamics-based formalism has been commonly used to analyzed prokaryotic gene regulation and its biological justification has been widely appreciated[32–34], this model simplification may alter system behavior and limit the applicability of the findings. However, qualitatively consistent results between our positive-feedback models and more general Gaussian-based models suggest minimal impact by such details of underlying gene regulation structures on a wider applicability of our results. Other potential limitations of the study arise from the dependency of the results on simulation settings. Although our analysis showed qualitatively consistent results under a range of evolutionary scenarios, the coverage was limited. Accordingly, our conclusion does not intend to rule out that some unexplored evolutionary scenarios favor reversion from the bistable to the monostable trait under stabilizing selection but rather lays out a plausible evolutionary scenario in which wild-type organisms can stably maintain their switching machinery during extended environmental stasis.

High gene expression stability facilitated by hidden switching mechanisms plays essential roles in development, including the normal functioning of the yeast galactose signaling network[35] and the *Xenopus* oocyte maturation decision network[36]. More recently, Raj et al.[10] observed that some mutations in the wild-type *Caenorhabditis elegans* intestinal development circuit resulted in a highly stochastic cell-fate decision, with some mutant embryos failing to develop intestinal cells, that activation of *elt-2*, the master regulator of intestinal differentiation, via its feedback-based bistable regulation was crucial to normal intestinal differentiation, and that mutations in upstream genes in this network can increase expression variability in *elt-2*, leading to abnormal development. Our results suggest the retention of such hidden switches to facilitate higher phenotypic stability under natural selection.

While our results indicated the advantages of high gene expression stability in static environments, the evolved stability levels were clearly limited by an upper bound. Because our gene circuit model captured the intrinsic fluctuations in gene expression and other sources of gene expression variability, the gene expression stability plateau observed in both ancient and derived populations may reflect the fundamental limit containing gene expression noise[37–39]. While the level of this limit depends on the specific structure of gene regulatory processes, the important physical constraint applicable to all biological systems—that some level of variability from intrinsic fluctuations is inevitable—is dealt with evolutionarily.

An increase in gene expression stability appears advantageous when the mean expression level is close to optimal and is positively

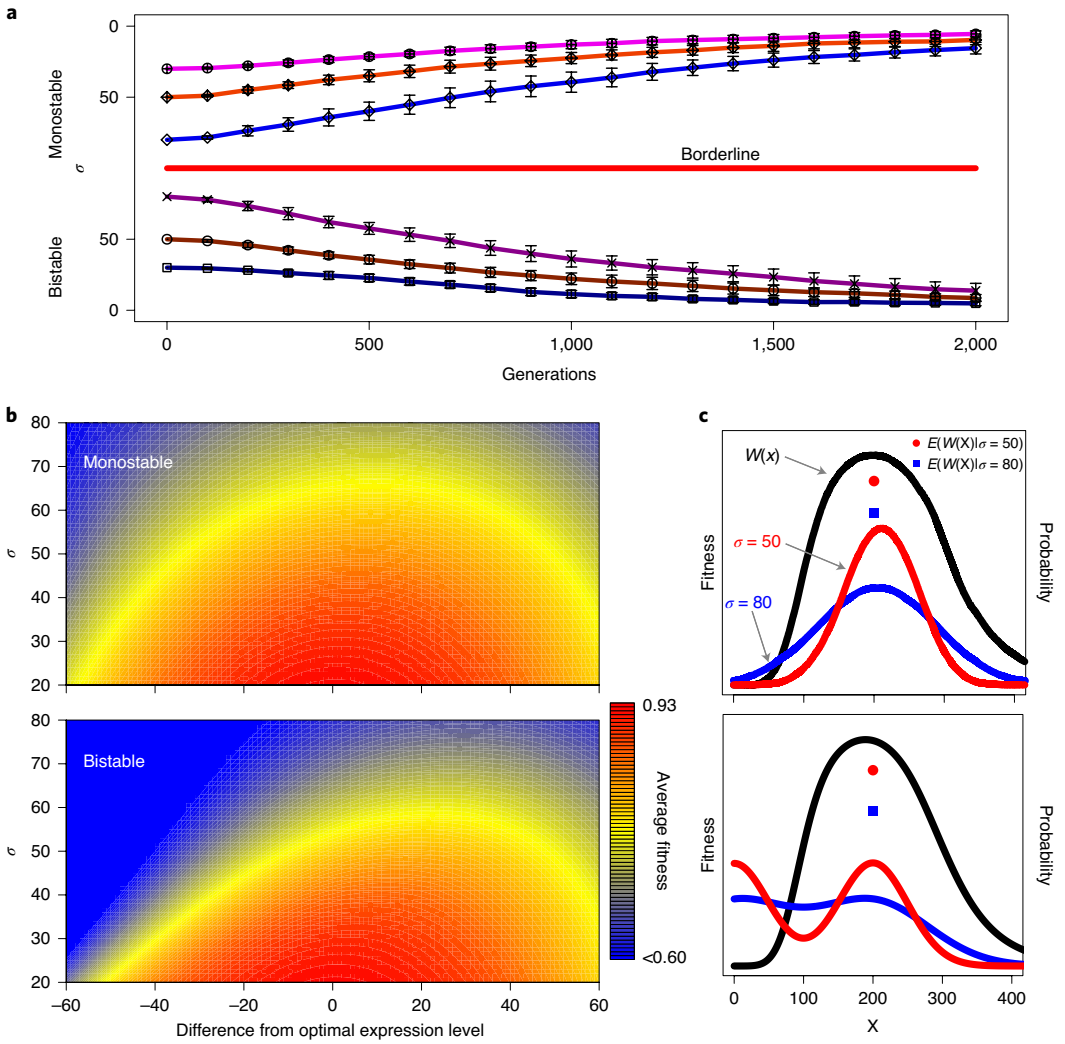

Fig. 4 | Evolutionary simulation results of Gaussian-based models. a, Average evolutionary trajectories of a Gaussian-based gene expression model. Evolution was simulated from a clonal population of either monostable individuals or bistable individuals. There were three different settings for the initial value of the Gaussian width (that is, gene expression stability): $\sigma = 30$, 50 and 80 (each with $n = 20$). Each point represents the mean of the mean Gaussian widths of the 20 runs, while each error bar represents the s.d. **b**, Heatmaps showing how the average fitness changes based on the Gaussian width and the distance of the high-expression stable state from the optimal gene expression level for the monostable model (top) and the bistable model (bottom). **c**, Difference in the average fitness based on different values of the Gaussian width for the monostable model (top) and the bistable model (bottom). The probability was computed using the corresponding density function with 0.1 as the internal length.

selected under natural selection. This does not contradict a previous study that considered the evolutionary scenario with the average gene expression level being fixed and far from optimal, concluding that higher levels of gene expression noise would be beneficial and selected for under stabilizing selection[31]. Our study investigated the evolution of gene expression processes that could adjust their mean expression level via mutational shifts. In our simulation, if the current gene expression level was far from optimal, evolution would select mutants that moved that level closer to optimal in the static environment. We focused more on the evolution of gene expression stability when the mean expression level was close to optimal, suggesting that gene expression stability plays different roles in adaptive evolution depending on the context. A recent experimental study in yeast confirmed that the effects of gene expression noise on fitness depends on the distance between the average and optimal protein abundance levels; higher noise levels are advantageous when the average protein level is far from optimal, whereas lower noise levels are advantageous when the average protein level is close to optimal[40].

We found that genotypes to express high-threshold bistable phenotypes were close to those expressing low-threshold ones. 'Hidden' bistable switches stably maintained in a population to buffer gene expression variability in a static environment can be reactivated via relatively small genetic changes in response to perturbations. Such phenotypic switching may play a crucial 'capacitor' role in unveiling cryptic genetic variations and facilitating the evolution of adaptive novelties[7,41]. Furthermore, the maintenance of hidden bistable switches can also facilitate atavisms[12]. Indeed, recent studies have reported the reversion of a phenotype that emerged from the evolution of a synthetic positive-feedback gene circuit with a stress-response function[42–44]. The researchers designed a bistable gene circuit to regulate a gene targeting a specific antibiotic[43] and evolved it in an environment without this antibiotic. Because of high gene expression metabolic costs, the derived gene circuits apparently lost their drug-resistant function; however, when the derived gene circuits were placed back into the antibiotic-containing environment, some were able to regain this function[44].

In 1942, Waddington used the term canalization to describe general observations that naturally selected organisms produce one definite end-product regardless of minor variations in conditions during the development[1]. Although this canalization model did not consider stochastic gene expression[4,5], recent single-cell studies revealed that the ability to control gene expression noise in wild-type organisms was essential to the constancy of developmental programmes and the complete penetrance of phenotypes[9,10]. Thus, regulation of gene expression noise crucially buffers underlying variations and facilitates developmental canalization of discrete phenotypes. This extended view of canalization explains the evolution of hidden threshold traits from stochastic switching traits and the maintenance of high-threshold bistable switches in naturally selected organisms during a long period of static environment.

Methods

Gene circuit model. Our gene circuit model for the expression of protein X comprised two variables, that is, m and x, which represent the molecule copy numbers of the mRNA and the protein forms, respectively, and four reaction processes, that is, transcription, mRNA degradation, translation and protein degradation. In Supplementary Section 3, we present the biological justification of the gene circuit model. We modeled our transcription process using a thermodynamics-based approach with the following kinetic law:

$$q(x) = a\left[\frac{k_b + k_a(x/K_d)^n}{1 + (x/K_d)^n}\right] \tag{1}$$

where parameters k_b and k_a are the basal and activated transcription rates, respectively, a is a scaling factor of these rates, and K_d and n represent the binding affinity and cooperativity, respectively.

The mRNA degradation process was modeled using a first-order reaction with kinetic law $k_{mdeg}m$, and the translation process was modeled using another first-order reaction with kinetic law $k_{trans}m$. The average number of the protein molecules produced from a single copy of mRNA transcript, then, is given by $b = k_{trans}/k_{mdeg}$. We modeled the protein degradation using a first-order reaction with kinetic law $k_{deg}x$. To simulate this gene circuit model for one cell generation, we ran Gillespie's stochastic simulation algorithm[46] for 2,000 s, which is within the range of typical bacterial generation time. In the stochastic simulation algorithm, the rate of the jth reaction, a_j, is defined so that the probability that this jth reaction will occur in the system within the next infinitesimal time dt is characterized by a_jdt.

To map the genetic makeup of each individual with its phenotype, we required an approach to obtain the dynamic property of the gene circuit model with a given parameter combination. With a continuum-state approximation, a stochastic process representing this gene circuit can be described by the following Fokker–Planck equation:

$$\begin{aligned}\frac{\partial p(x,t)}{\partial t} &= -\frac{\partial}{\partial x}\left\{\left[bq(x) - k_{deg}x\right]p(x,t)\right\} \\ &+ \frac{1}{2}\frac{\partial^2}{\partial x^2}\left\{\left[(2b^2 + b)q(x) + k_{deg}x\right]p(x,t)\right\}\end{aligned} \tag{2}$$

where $p(x,t)$ is the probability density function of $X(t)$ (see Supplementary Section 4 for the derivation of this Fokker–Planck equation). From this equation, the time-invariant probability density of the protein abundance level in the stationary regime, $p_s(x)$, is given by

$$p_s(x) = \frac{C}{(2b^2 + b)q(x) + k_{deg}x}\exp[-\phi(x)], \tag{3}$$

where

$$\phi(x) = -2\int_0^x \frac{bq(x') - k_{deg}x'}{(2b^2 + b)q(x') + k_{deg}x'}\mathrm{d}x', \tag{4}$$

with C being a normalization constant and $\phi(x)$ being the potential function. By approximating dx by a small but finite Δx, this equation can be used to map parameters to the protein abundance distribution without performing stochastic simulations.

Evolutionary simulation. As described in Results, we simulated the evolution of 1,000 individuals with this gene circuit for 30,000 generations under each of three different conditions consecutively. That is, during the first 30,000 generations, the population was evolved in environment E_1; during the second 30,000 generations, it was evolved in a fluctuating condition under which the environment switches between E_0 and E_1 every 20 generations; and during the last 30,000 generations, the population was evolved in environment E_1. In this simulation, we set $k_b = 0.02$, $k_a = 0.2$, $k_{mdeg} = 0.1$, $k_{deg} = 0.002$, and a, b, K_d and n as evolvable. For the individuals in the founding population, these evolvable parameters were set as follows: $a = 1$, $b = 1$ (that is, $k_{trans} = 0.1$), $K_d = 50$ and $n = 0$, each having a gene expression process with a constitutive promoter without feedback loop regulation. We captured genetic mutations by adding small perturbations to the evolvable parameters. Specifically, we first modeled perturbations in a, b, K_d and n using random variates from zero-mean Gaussian distributions with the Gaussian width σ being 0.2, 0.2, 1.0 and 0.2, respectively. In our follow-up simulations, we changed this perturbation setting to check the consistency of our results (Supplementary Figs. 7 and 8).

The fitness of individuals depends on their environment, and we studied two fitness functions, W_0 and W_1, for environments E_0 and E_1, respectively. These functions have the following forms:

$$W_0(x) = 1 - \frac{(x/x_\theta)^5}{1 + (x/x_\theta)^5}, \tag{5}$$

$$W_1(x) = \frac{(x/x_\theta)^5}{1 + (x/x_\theta)^5} - \frac{(x/x_c)^2}{1 + (x/x_c)^2}, \tag{6}$$

where x_θ is set to 50 and x_c is set to 1,000. In environment E_0, the optimal protein level, μ_{low}, is 0, while in environment E_1, the optimal level, μ_{high}, is 135.

To test whether our main results were not specific to the fitness function used, we performed evolutionary simulations with the following fitness functions (Supplementary Fig. 6):

$$W_0(x) = \exp\left(\frac{-(x - \mu_{low})^2}{2s^2}\right) \tag{7}$$

$$W_1(x) = \exp\left(\frac{-\left(x - \mu_{high}\right)^2}{2s^2}\right) \tag{8}$$

where μ_{low} (the optimal gene expression level for E_0), μ_{high} (the optimal gene expression level for E_1) and s (the Gaussian width) were set to 0, 15 and 85, respectively.

Selection of individuals for a new generation was modeled using roulette wheel selection. To select each of 1,000 individuals for the new population, the normalized fitness over all individuals in the current population was used as the probability distribution for the selection, and each individual for the new generation was randomly picked from this distribution.

Classification of bistability and monostability. To classify each individual in the population as a bistable or monostable gene expression phenotype, we searched for the number of local extrema in $p_s(x)$. Because the sufficient condition to have either a stable state (that is, protein level at which $p_s(x)$ has a peak) or an unstable state (that is, protein level at which $p_s(x)$ has a bottom) is that $p_s'(x) = 0$, we computed the number of roots of $p_s'(x)$. The first derivative of $p_s(x)$ can be expressed as

$$p_s'(x) = \frac{\alpha(x)}{(2b^2 + b)q(x) + k_{deg}x}p_s(x), \tag{9}$$

where

$$\alpha(x) = 2bq(x) - 2k_{deg}x - \left(2b^2 + b\right)q'(x) - k_{deg}. \tag{10}$$

From this equation, we can see that stable and unstable steady states must be roots of $\alpha(x)$.

We used a root-finding method to find the number of steady states and to classify whether a given genotype encoded a monostable gene expression process or a bistable gene expression process. With the boundary between 0 and 1,000, we first counted the number of roots of $\alpha(x)$ for each individual. Because we were interested in 'functional' phenotypic switches, we considered only those bistable systems with a higher-expression stable state being higher than threshold x_θ. Thus, if an individual had two roots of $\alpha(x)$ with the higher one being larger than x_θ (that is, the higher-expression stable state is higher than x_θ and the lower-expression attractor state is 0), then we considered this as bistable. In addition, if an individual had at least three roots with the third smallest root being larger than x_θ (that is, the higher-expression stable state is higher than x_θ), then we considered this as bistable. If a given individual did not satisfy either of these two bistable conditions, then we considered this individual as monostable.

Note that this Fokker–Planck model-based stochastic bistability prediction does not always produce consistent results with the deterministic counterpart. This is because the continuous-deterministic treatment ignores the diffusion term, giving rise to deviations from the continuous-stochastic prediction[39,47]. These differences can be substantial, for example, when the effects of translational bursting on the steady-state behavior are large. Supplementary Fig. 18 illustrates differences between our bistability prediction and the deterministic counterpart.

Stability measure. To quantify the stability of the individuals in the ancient and the derived populations, we approximated the shape of $p_s(x)$ around the higher-expression stable state x_{hs} by a Gaussian function $g(x)$ (ref. [39]) where

$$g(x) = p_s(x_{hs})\exp\left[\frac{-(x-x_{hs})^2}{2w^2}\right]. \quad (11)$$

To obtain the value of width w, we set a constraint that required $g''(x_{hs}) = p_s''(x_{hs})$, that is, the concavity around the higher-expression stable state was set to be the same between the two functions. With this constraint, we could express w as

$$w = \sqrt{\frac{-(2b^2+b)q(x_{hs}) - k_{deg}x_{hs}}{\alpha'(x_{hs})}}. \quad (12)$$

Then, for each individual with $x_{hs} > x_\theta$, the stability of its gene expression process for the environment under which higher expression of protein X was favored is given by x_{hs}/w. Thus, the higher this value is, the higher the gene expression stability around the higher-expression stable state.

Evolution with a Gaussian-based gene expression model. To analyze whether the maintenance of bistable traits was specific to the autoregulation gene expression model that we used or whether the phenomenon was more general, we used a gene expression model with a higher level of abstraction. In this abstracted model, we had two discrete-time stationary processes, $X_M(g)$ and $X_B(g)$, to represent the protein abundance levels of a monostable individual and a bistable individual at generation g, respectively. The probability density function of X_M is denoted by $f_M(x)$, which is defined as follows:

$$f_M(x) = \begin{cases} \frac{C}{\sigma\sqrt{2\pi}}e^{-\frac{(x-\mu_H)^2}{2\sigma^2}}, & \text{if } x \geq 0, \\ 0, & \text{otherwise.} \end{cases} \quad (13)$$

where C is the normalization constant, σ is the Gaussian width controlling the gene expression noise and μ_H is the higher-expression stable state.

In contrast, the probability density function of X_B is bimodal which is based on two Gaussian distributions $f_L(x)$ and $f_H(x)$. If the protein abundance level at the previous generation, x', is less than x_θ, then the distribution $f_L(x)$ is used to sample X. Otherwise (that is, if $x' \geq x_\theta$), then, the distribution $f_H(x)$ is used to sample X. That is, f_L is the distribution for the lower-expression valley and f_H is the distribution for the higher-expression one. Because the optimal expression level in the lower-expression valley was 0, we set $f_L(x)$ to be the following half-normal density:

$$f_L(x) = \begin{cases} \frac{C\sqrt{2}}{\sigma\sqrt{\pi}}e^{-\frac{x^2}{2\sigma^2}}, & \text{if } x \geq 0, \\ 0, & \text{otherwise.} \end{cases} \quad (14)$$

In the higher-expression region, the optimal expression level was the same as the monostable case, so we set $f_H(x)$ to be the following Gaussian density function:

$$f_H(x) = \begin{cases} \frac{C}{\sigma\sqrt{2\pi}}e^{-\frac{(x-\mu_H)^2}{2\sigma^2}}, & \text{if } x \geq 0, \\ 0, & \text{otherwise.} \end{cases} \quad (15)$$

Thus, by using these two density functions, we defined $f_B(x|x')$, the density function for $X_B(g+1) = x$ given that $X_B(g) = x'$ as follows:

$$f_B(x|x') = \begin{cases} f_L(x), & \text{if } x' < x_\theta, \\ f_H(x), & \text{otherwise.} \end{cases} \quad (16)$$

With this definition of the bistable probability distribution, if the protein level at the previous generation was at least x_θ, the two probability density functions, $f_M(x)$ and $f_B(x|x')$, became identical for this generation. On the contrary, if the protein level at the previous generation was lower than the threshold, the half-Gaussian distribution with the lower-expression stable state (that is, $f_L(x)$) was used. Thus, $f_B(x|x')$ had two Gaussian distributions separated by a barrier at $x = x_\theta$. Let L and H be the lower- and higher-expression regions, respectively, that is, $L = [0, x_\theta)$ and $H = [x_\theta, \infty)$. On this basis, the probability to spontaneously transition from H to L was given by

$$p_{H\to L} = \int_0^{x_\theta} f_H(x)dx, \quad (17)$$

while the probability to spontaneously transition from L to H was given by

$$p_{L\to H} = \int_{x_\theta}^{\infty} f_{L(x)}dx. \quad (18)$$

In the simulation reported in the main text (Fig. 4a), we set the value of μ_H and x_θ to 200 and 100, respectively.

In this gene expression model, the only evolvable parameter was for the Gaussian width σ. We captured transitions between the monostable and bistable traits using the evolvable parameter σ'. Specifically, we set the threshold for the Gaussian width σ_θ so that whenever σ' became higher than this threshold, we switched the trait to the other one. We set the value of σ_θ to 100 so that transitions occur when the potential function became flat—that is, when the gene expression stability became very low. A mutation in σ' was modeled by adding Ξ_σ, a zero-mean Gaussian random variable, to σ'. To have gradual changes in the level of gene expression stability, the standard deviation of Ξ_σ was set to 2. Using σ', we expressed $\sigma_i(g)$, the Gaussian width of the ith individual at generation, as:

$$\sigma_i(g) = \begin{cases} \sigma_i'(g), & \text{if } \sigma_i'(g) < \sigma_\theta, \\ 2\sigma_\theta - \sigma_i'(g), & \text{otherwise.} \end{cases} \quad (19)$$

In this simulation, the environment was assumed to be static and to always favor individuals with higher protein levels. To compute the fitness of each individual, we used the following function

$$W(x) = \frac{(x/x_\theta)^h}{1+(x/x_\theta)^h} - \frac{(x/x_c)^8}{1+(x/x_c)^8} \quad (20)$$

where h was set to 5 in the simulation reported in the main text, and in the follow-up simulation it was also set to 1 (Supplementary Fig. 15). With $h = 5$, the optimal gene expression level was around 189, which is close to μ_H. We further performed simulations with a different form of this fitness function. Specifically, we used the following Gaussian-based fitness function

$$W(x) = e^{-\frac{(x-m)^2}{2s^2}}, \quad (21)$$

where m and s were changed to take several values (Supplementary Fig. 16).

The number of individuals in the population was fixed to be 1,000, and the mutation rate of the Gaussian width per individual per generation was set to be 0.01. We used the roulette wheel selection to model the selection of individuals.

Statistics. *Association of parameters among evolved populations.* Pearson's correlation coefficient and the distribution of evolved parameters were computed using the most common parameter combination in the evolved populations ($n = 200$) in the three environmental phases. Evolved populations were chosen to be in E_1, and they were from the 30,000th, 29,900th and 30,000th generations for the ancient, intermediate and derived environmental phases, respectively.

Significance of bistable trait in the derived population. P value to show the significance of the prevalence of the bistable trait in the derived population over the ancient one was computed using the fisher.test function in R (version 3.5.2) with the 'alternative' parameter set to 'two.sided' on the data from all simulation runs ($n = 200$) at generation 30,000.

Odds ratio for association between intermediate and derived populations. The OR and the associated 95% CI to show the significance of the association of bistability between the intermediate and derived populations were computed by constructing the confusion matrix shown in Fig. 2c ($n = 200$) and applying it to the fisher.test function in R.

Error bars. In Fig. 3a, for each generation point, the error bar represents the s.e. of the mean gene expression stability of the populations ($n = 200$). This s.e. was computed using populations, each of which has a valid mean stability of the high-expression stable state from 1,000 individuals. Thus, the s.e. at generation 0 of the derived population was computed using 143 samples.

In Fig. 4a, for each data point, the error bar represents the s.d. of the mean Gaussian width of 1,000 individuals of each of the simulation runs ($n = 20$).

Data availability

The simulation data along with the data analysis scripts associated with the current submission and the source data for Figs. 1–4 are available in the Zenodo repository[48].

Code availability

The simulator source code and data analysis scripts have been deposited in GitHub, and they can be accessed at https://github.com/hkuwahara/evo-hidden-switch. The tool package has also been deposited in Zenodo[48].

Received: 30 May 2020; Accepted: 2 November 2020;
Published online: 14 January 2021

References

1. Waddington, C. H. Canalization of development and the inheritance of acquired characters. *Nature* **150**, 563–565 (1942).

2. Waddington, C. H. Genetic assimilation of an acquired character. *Evolution* **7**, 118–126 (1953).
3. Schmalhausen I. I., Dordick I. & Dobzhansky T. *Factors of Evolution: The Theory of Stabilizing Selection* (Univ. Chicago Press, 1987).
4. Gibson, G. & Wagner, G. Canalization in evolutionary genetics: a stabilizing theory? *Bioessays* **22**, 372–380 (2000).
5. West-Eberhard, M. J. Toward a modern revival of Darwin's theory of evolutionary novelty. *Phil. Sci.* **75**, 899–908 (2008).
6. Félix, M. A. & Barkoulas, M. Pervasive robustness in biological systems. *Nat. Rev. Genet.* **16**, 483–496 (2015).
7. West-Eberhard, M. J. Phenotypic plasticity and the origins of diversity. *Annu. Rev. Ecol. Syst.* **20**, 249–278 (1989).
8. Suzuki, Y. & Nijhout, H. F. Evolution of a polyphenism by genetic accommodation. *Science* **311**, 650–652 (2006).
9. Eldar, A. et al. Partial penetrance facilitates developmental evolution in bacteria. *Nature* **460**, 510–514 (2009).
10. Raj, A., Rifkin, S. A., Andersen, E. & van Oudenaarden, A. Variability in gene expression underlies incomplete penetrance. *Nature* **463**, 913–918 (2010).
11. Specchia, V. et al. Hsp90 prevents phenotypic variation by suppressing the mutagenic activity of transposons. *Nature* **463**, 662–665 (2010).
12. West-Eberhard, M. J. *Developmental Plasticity and Evolution* (Oxford Univ. Press, 2003).
13. Masel, J., King, O. D. & Maughan, H. The loss of adaptive plasticity during long periods of environmental stasis. *Am. Nat.* **169**, 38–46 (2007).
14. Kærn, M., Elston, T., Blake, W. & Collins, J. Stochasticity in gene expression: from theories to phenotypes. *Nat. Rev. Genet.* **6**, 451–464 (2005).
15. Raser, J. M. & O'Shea, E. K. Noise in gene expression: origins, consequences, and control. *Science* **309**, 2010–2013 (2005).
16. Losick, R. & Desplan, C. Stochasticity and cell fate. *Science* **320**, 65–68 (2008).
17. Raj, A. & van Oudenaarden, A. Nature, nurture, or chance: stochastic gene expression and its consequences. *Cell* **135**, 216–226 (2008).
18. Acar, M., Mettetal, J. T. & van Oudenaarden, A. Stochastic switching as a survival strategy in fluctuating environments. *Nat. Genet.* **40**, 471–475 (2008).
19. Capp, J. P. Noise-driven heterogeneity in the rate of genetic-variant generation as a basis for evolvability. *Genetics* **185**, 395–404 (2010).
20. Johnston, R. J. Jr & Desplan, C. Stochastic mechanisms of cell fate specification that yield random or robust outcomes. *Annu. Rev. Cell Dev. Biol.* **26**, 689–719 (2010).
21. Kuwahara, H. & Soyer, O. S. Bistability in feedback circuits as a byproduct of evolution of evolvability. *Mol. Syst. Biol.* **8**, 564 (2012).
22. Becskei, A., Séraphin, B. & Serrano, L. Positive feedback in eukaryotic gene networks: cell differentiation by graded to binary response conversion. *EMBO J.* **20**, 2528–2535 (2001).
23. Thattai, M. & Van Oudenaarden, A. Stochastic gene expression in fluctuating environments. *Genetics* **167**, 523–530 (2004).
24. Salathé, M., Van Cleve, J. & Feldman, M. W. Evolution of stochastic switching rates in asymmetric fitness landscapes. *Genetics* **182**, 1159–1164 (2009).
25. Balázsi, G., van Oudenaarden, A. & Collins, J. J. Cellular decision making and biological noise: from microbes to mammals. *Cell* **144**, 910–925 (2011).
26. Liberman, U., Van Cleve, J. & Feldman, M. W. On the evolution of mutation in changing environments: recombination and phenotypic switching. *Genetics* **187**, 837–851 (2011).
27. Bedford, T. & Hartl, D. L. Optimization of gene expression by natural selection. *Proc. Natl Acad. Sci. USA* **106**, 1133–1138 (2009).
28. Ozbudak, E. M., Thattai, M., Kurtser, I., Grossman, A. D. & van Oudenaarden, A. Regulation of noise in the expression of a single gene. *Nat. Genet.* **31**, 69–73 (2002).
29. Lachmann, M. & Jablonka, E. The inheritance of phenotypes: an adaptation to fluctuating environments. *J. Theor. Biol.* **181**, 1–9 (1996).
30. Meyers, L. A., Ancel, F. D. & Lachmann, M. Evolution of genetic potential. *PLoS Comput. Biol.* **1**, 236–243. (2005).
31. Zhang, Z., Qian, W. & Zhang, J. Positive selection for elevated gene expression noise in yeast. *Mol. Syst. Biol.* **5**, 299 (2009).
32. Bintu, L. et al. Transcriptional regulation by the numbers: models. *Curr. Opin. Genet. Dev.* **15**, 116–124 (2005).
33. Kuwahara, H. et al. in *Transactions on Computational Systems Biology VI* (eds Priami, C. & Plotkin, G.) 150–175 (Springer, 2006).
34. Gunawardena, J. Time-scale separation—Michaelis and Menten's old idea, still bearing fruit. *FEBS J.* **281**, 473–488 (2014).
35. Acar, M., Becskei, A. & van Oudenaarden, A. Enhancement of cellular memory by reducing stochastic transitions. *Nature* **435**, 228–232 (2005).
36. Xiong, W. & Ferrell, J. E. Jr A positive-feedback-based bistable'memory module' that governs a cell fate decision. *Nature* **426**, 460–465 (2003).
37. Lestas, I., Vinnicombe, G. & Paulsson, J. Fundamental limits on the suppression of molecular fluctuations. *Nature* **467**, 174–178 (2010).
38. Thattai, M. & van Oudenaarden, A. Intrinsic noise in gene regulatory networks. *Proc. Natl Acad. Sci. USA* **98**, 8614–8619 (2001).
39. Kuwahara, H., Arold, S. T. & Gao, X. Beyond initiation-limited translational bursting: the effects of burst size distributions on the stability of gene expression. *Integr. Biol.* **7**, 1622–1632 (2015).
40. Duveau, F. et al. Fitness effects of altering gene expression noise in *Saccharomyces cerevisiae*. *eLife* **7**, e37272 (2018).
41. Gibson, G. & Dworkin, I. Uncovering cryptic genetic variation. *Nat. Rev. Genet.* **5**, 681–690 (2004).
42. Nevozhay, D., Adams, R. M., Van Itallie, E., Bennett, M. R. & Balázsi, G. Mapping the environmental fitness landscape of a synthetic gene circuit. *PLoS Comput. Biol.* **8**, e1002480 (2012).
43. González, C. et al. Stress-response balance drives the evolution of a network module and its host genome. *Mol. Syst. Biol.* **11**, 827 (2015).
44. Kheir Gouda, M., Manhart, M. & Balázsi, G. Evolutionary regain of lost gene circuit function. *Proc. Natl Acad. Sci. USA* **116**, 25162–25171 (2019).
45. Pujadas, E. & Feinberg, A. P. Regulated noise in the epigenetic landscape of development and disease. *Cell* **148**, 1123–1131 (2012).
46. Gillespie, D. T. Exact stochastic simulation of coupled chemical reactions. *J. Phys. Chem.* **81**, 2340–2361 (1977).
47. Friedman, N., Cai, L. & Xie, X. S. Linking stochastic dynamics to population distribution: an analytical framework of gene expression. *Phys. Rev. Lett.* **97**, 168302 (2006).
48. Kuwahara, H. Simulation tool and data analysis scripts for the study of stable maintenance of bistable switch under static environments (version 0.16). *Zenodo* https://doi.org/10.5281/zenodo.4120179 (2020).

Acknowledgements

We thank O. Soyer and T. Gojobori for their comments on an earlier version of the manuscript. X.G. was supported by the King Abdullah University of Science and Technology (KAUST) Office of Sponsored Research (OSR) under award numbers BAS/1/1624-01, URF/1/3412-01, URF/1/3450-01, FCC/1/1976-18, FCC/1/1976-23, FCC/1/1976-25, FCC/1/1976-26 and FCS/1/4102-02.

Author contributions

H.K. conceived and designed the study, developed tools, performed analysis and wrote the paper. X.G. oversaw the project and wrote the paper. All authors reviewed the final manuscript.

Competing interests

The authors declare no competing interests.

Additional information

Supplementary information is available for this paper at https://doi.org/10.1038/s43588-020-00001-y.

Correspondence and requests for materials should be addressed to X.G.

Peer review information *Nature Computational Science* thanks Gábor Balázsi and Xiaojun Tian for their contribution to the peer review of this work. Fernando Chirigati was the primary editor on this article and managed its editorial process and peer review in collaboration with the rest of the editorial team.

Reprints and permissions information is available at www.nature.com/reprints.

Publisher's note Springer Nature remains neutral with regard to jurisdictional claims in published maps and institutional affiliations.